


Nonequilibrium quantum phase transition in a spinor quantum gas in a lattice coupled to a membrane

Xingran Xu,^{1,2,3} Zhidong Zhang,^{2,3} and Zhaoxin Liang^{1,*}

¹*Department of Physics, Zhejiang Normal University, Jinhua 321004, China*

²*Shenyang National Laboratory for Materials Science, Institute of Metal Research, Chinese Academy of Sciences, Shenyang 110016, China*

³*School of Materials Science and Engineering, University of Science and Technology of China, Hefei 230026, China*

 (Received 1 May 2019; revised manuscript received 23 September 2019; published 19 November 2019)

Recently, a novel kind of hybrid atom-optomechanical system, consisting of atoms in a lattice coupled to a membrane, has been experimentally realized [A. Vochezer *et al.*, *Phys. Rev. Lett.* **120**, 073602 (2018)], which promises a viable contender in the competitive field of simulating nonequilibrium many-body physics. Here we are motivated to investigate a spinor Bose gas coupled to a vibrational mode of a nanomembrane, focusing on analyzing the role of the spinor degrees of freedom therein. Through an adiabatic elimination of the degrees of freedom of the quantum oscillator, we derive an effective Hamiltonian which reveals a competition between the force localizing the atoms and the membrane displacement. We analyze the dynamical stability of the steady state using the Bogoliubov–de Gennes approach and derive the stationary phase diagram in the parameter space. Then, we investigate the first-order nonequilibrium quantum phase transition (NQPT) from a localized symmetric state of the atom cloud to a shifted symmetry-broken state, characterized by the occurrence of a hysteresis. Moreover we present a detailed analysis of the effects of the spin degree of freedom on NQPT. Our work presents a simple way to study the effects of the spinor degree of freedom on the nonequilibrium nonlinear phenomena that is complementary to ongoing experiments on the hybrid atom-optomechanical system.

DOI: [10.1103/PhysRevA.100.053616](https://doi.org/10.1103/PhysRevA.100.053616)

I. INTRODUCTION

In recent years, the hybrid atom-optomechanical systems [1–5], where a membrane is coupled to ultracold quantum gases, have attracted considerable interest as a novel and versatile alternative to more conventional optomechanical setups. Combining mechanical oscillators and ultracold atoms, such hybrid systems [1–10] provide opportunities for cooling, detection, and quantum control of mechanical motion, with applications in precision sensing, quantum-level signal transduction, as well as for fundamental tests of quantum mechanics [11–15]. For example, state-of-the-art optomechanics is nowadays able to realize optical feedback cooling of the mechanical oscillator to its quantum-mechanical ground state [3]. Being intrinsically nonequilibrium, such a hybrid mechanical atomic system further provides a natural setting for nonequilibrium many-body quantum systems [5,16]. Adding phononic degrees of freedom to the optical lattice toolbox [17,18], it also opens new routes to mimic the lattice vibrations and quantum simulations of phonon dynamics in realistic solid materials [16].

Building on the above development, further accounts of the spinor degree of freedom of the atom part [9,19], which is a key ingredient playing out in modern physics, are expected to reveal exceptionally rich physics in hybrid atom-optomechanical systems. In this work, we are motivated to study a spinor hybrid atom-optomechanical setup that consists

of a membrane coupled to spinor ultracold quantum gases. There, the light-mediated coupling between the atoms and the membrane is nonresonant, allowing for adiabatic elimination of the degree of freedom of the quantum oscillator. The resulting Hamiltonian can be regarded as a nonlinear quantum system in periodic potentials. Solving the Bogoliubov–de Gennes equations, we derive the dynamical stability phase diagram for this system in the parameter space. As the atom-membrane coupling is tuned via controlling the laser intensity, a first-order nonequilibrium quantum phase transition (NQPT), characterized by the occurrence of a hysteresis, is induced between a localized symmetric state and a symmetry-broken quantum many-body state exhibiting a shifted cloud-membrane configuration. Finally, we discuss how the stationary-state phase can be probed through the elementary excitations of the model system. We believe our model provides a simple way to study the nonequilibrium nonlinear phenomena that is complementary to ongoing experiments on the hybrid atom-optomechanical systems.

The emphasis and value of the present work are to provide a theoretical model, i.e., an extended two-component Gross-Pitaevskii equation coupled to a quantum harmonic oscillator in describing the hybrid mechanical-atomic system, which at the mean-field level captures the key physics regarding the interplay of quantum many-body physics, nonequilibrium nature, and the spinor degree of freedom. Our study builds on recent progress in engineering the optomechanical coupling λ in experiments [1,2]. For vanishing intrinsic optomechanical coupling $\lambda \rightarrow 0$, our model reduces to the equilibrium two-component condensates which have been intensively explored

*Corresponding author: zhliang@gmail.com

both theoretically and experimentally in the context of ultracold quantum gases [20–22]. Note that our previous work [16] has obtained the steady-state phase diagram for the *one-component* hybrid mechanical-atomic system, which has extended studies on the steady-state phases from the superfluid regime [5] into the full parameter regimes. In this work, we together with Ref. [19] further account for the spinor degree of freedom of the atom part. These four working together will provide a complete description of the steady-state phase diagram of the hybrid mechanical-atomic system experimentally motivated by Refs. [1,2]. We hope the theoretical model proposed in this work can serve as an alternative model to study the spinor nonequilibrium nonlinear phenomena in a highly controllable way.

The paper is organized as follows. In Sec. II, we briefly describe the model system and corresponding mean-field treatment. In Sec. III, we revisit the dynamical stability analysis of the stationary state using the Bogoliubov–de Gennes approach and derive the dynamical stability phase diagram of the model system in the parameter space. Section IV presents a detailed analysis of the nonequilibrium quantum phase transition, in particular, the role of the spinor nature of the atomic gas on the quantum phase. The hysteresis and Landau expansion analyses are presented in Sec. V and elementary excitation is calculated in Sec. VI. Finally, we conclude in Sec. VII.

II. MODEL HAMILTONIAN

In this work, we consider a spinor hybrid mechanical-atomic system consisting of a membrane in a single-sided optical cavity, i.e., one mirror of the cavity is designed to reflect incident light on resonance and forms a standing wave in front of the cavity, in which a spinor Bose-Einstein condensate (BEC) can be trapped. Our setup is of immediate relevance in the context of experiments for the one-component hybrid mechanical-atomic system [1–4]. Furthermore, the spin degree of freedom can be encoded by two atomic internal states or sublattices [20]. Our goal is to find a nonequilibrium quantum phase transition from a localized symmetric state of the atom to a shifted symmetry-broken, in particular, focus on the spin degree of freedom’s effects on the phase transition.

The atom part of our model consists of a two-component BEC in a spin-dependent optical superlattice [23,24] along the x direction, whereas the model system is uniform in the other two directions. To be specific, we choose the internal states of $|F = 1, m = -1\rangle$ and $|F = 2, m = -2\rangle$ of the atom ^{87}Rb as a pseudo-spin-1/2 system. The one-dimensional spin-dependent optical superlattice is formed by superimposing two optical standing waves, which can be written as $V(x) = V_1 \sin^2(k_1x) + V_2 \sin^2(k_2x + \phi)$. We remark that the spin-dependent optical superlattice can allow one to coherently address and manipulate each component of the spinor BEC independently. Furthermore, we are interested in the scenario of only one component of a spinor BEC coupling to a micromechanical membrane. Such kind of coupling mechanism can be understood as follows. The displacement $X(t)$ of a micromechanical membrane provides a time-dependent boundary condition for one of the electromagnetic field [7,9] of $E \sim \sin[k(x - X)]$, but does not affect another electromagnetic field of creating an optical lattice. Then a displacement

of the membrane by an amplitude X leads to a phase shift $\delta\phi \sim FX/\lambda_L$ of the reflected light. Here, F stands for the finesse of the cavity and λ_L is the wavelength of the laser light. Due to the phase shift of the standing wave, a single atom trapped in an optical lattice of $V_2 \sin^2(k_2x + \phi + \delta\phi)$ is expected to experience a force $\propto \delta\phi$. Meanwhile, the atoms trapped in the lattice of $V_1 \sin^2(k_1x)$ are expected to be unaffected. This suggests that the coupling to the mechanical motion only affects a single spinor state. For the pure sake of the simplified calculations, we limit ourselves into the case of spin-dependent optical superlattice having the same period by letting $k_1 = k_2$. We remark that Ref. [9] has considered the case of the mechanical motion coupling to both components of a spinor BEC. At last, the freedom along the y and z directions decouples from the x direction, leading to the realization of a quasi-one-dimensional geometry.

Within the mean-field approximation [5,19], the order parameter for the condensate can be described by a two-component time-dependent wave function $\Psi = [\psi_1, \psi_2]^T$, in which the dynamics can be well described by the two-component Gross-Pitaevskii (GP) equations, i.e.,

$$i\hbar \frac{\partial}{\partial t} \psi_1 = -\hbar\omega_R \partial_x^2 \psi_1 + V \sin^2(x) \psi_1 + \hbar\Omega \psi_2 + gN |\psi_1|^2 \psi_1 + g_{12}N |\psi_2|^2 \psi_1 - 2\sqrt{N}\lambda\alpha_1 \sin(2x) \psi_1, \quad (1)$$

$$i\hbar \frac{\partial}{\partial t} \psi_2 = -\hbar\omega_R \partial_x^2 \psi_2 + V \sin^2(x) \psi_2 + \hbar\Omega \psi_1 + gN |\psi_2|^2 \psi_2 + g_{12}N |\psi_1|^2 \psi_2, \quad (2)$$

with V being lattice potential strength, N the number of the condensed atoms, $\hbar\omega_R$ is the kinetic energy, Ω denotes Rabi frequency, and g and g_{12} label interatomic and intra-atomic interactions, respectively. Here, the coupling between the atoms and the membrane labeled by λ can be obtained with a Born-Markov approximation by adiabatically eliminating the light field [5,16]. The α_1 is referred to the real part of the complex amplitude α of a coherent state [see Eq. (3)]. Note that going beyond the GP Eqs. (1) and (2) to fully include the quantum and thermal fluctuations of the quantum field is beyond the scope of this work.

The motion of the membrane can be treated as a one-dimensional quantum oscillator with frequency Ω , $H_m = \hbar\Omega_m a^\dagger a$ [5,16]. Within the mean-field framework, we are interested in the dynamics of the mean value of the field operator a under the coherent ansatz $\langle a \rangle = \alpha$. The equation of motion of α can be written as

$$i \frac{\partial}{\partial t} \alpha = (\Omega_m - i\gamma) \alpha - \sqrt{N}\lambda \int dx \sin(2x) |\psi_1|^2. \quad (3)$$

Here the γ represents a phenomenological damping rate and the membrane is coupled to one component of the two-component BEC. Note that $\alpha = \alpha_1 + i\alpha_2$ in Eq. (3) is a complex number (α_1 and α_2 being its real and imaginary part, respectively) and plays the role of the order parameter for the membrane. The physical meaning of α can be regarded as the displacement of the membrane around its equilibrium. In more detail, $\alpha = 0$ denotes an incoherent vibration

state of the membrane, whereas $\alpha \neq 0$ denotes a coherent vibration.

The stationary-state phase diagram of the spinor hybrid atom-optomechanical system described by Eqs. (1) and (2) is determined by five parameters: the lattice strength V , the coupling constant λ between the atom and membrane, the inter- and intra-atomic interactions g and g_{12} , and the Rabi frequency Ω . Note that there is a quantum phase transition for $\lambda = 0$ in the context of equilibrium ultracold atomic BEC [25] and dissipative polariton BEC [26]: $g_{12} > g + 2\Omega/n$ the system turns from an unpolarized phase to a polarized phase for order parameter $\langle \sigma_z \rangle = n_1 - n_2$ is zero or nonzero. In what follows, we address how the nonequilibrium nature of the model system, i.e., $\lambda \neq 0$, can affect the above quantum phase transition.

To motivate our discussion of effects of the spinor degree of freedom on the phase transition, one notices two important features with respect to the framework of Ref. [5]: First, the spinor degree of freedom of our model system is encoded in the two-component order parameters $[\psi_1, \psi_2]$; second, the membrane is coupled to the superposition of both the density and spin density of the BEC, which will inevitably couple to excitations in the density and spin-density fluctuations. This further justifies our motivation of focusing on the effects of the spinor degree of freedom on the phase transition.

From Eqs. (1) and (2), the key physical picture behind the nonequilibrium quantum phase transition can immediately be stated as follows: there exist two different kinds of periodic potentials, which dynamically compete with each other, depending on the backaction of the membrane on the atoms, and thus on the collective behavior of the atoms. We are interested in the tight-binding limit, where the lattice is so strong that the BEC system can be considered as a chain of trapped BECs that are weakly linked.

III. STABILITY OF THE HYBRID MECHANICAL-ATOMIC SYSTEM

The main goal of this work is to investigate the nonequilibrium quantum phase transition in a spinor quantum gas in a lattice coupled to a membrane. Before proceeding, we remark that the stationary states of a periodically trapped quantum gas is represented by a Bloch wave [27,28], i.e., a plane wave with periodic modulation of the amplitude. One unique feature in the system of the quantum gas in optical lattices coupled to a membrane is dynamical instability [27,29], which does not exist in the absence of either atomic interaction. In more detail, some of the Bloch waves can be dynamically unstable against certain perturbation modes q only when both factors are present. By dynamical instability, we mean that small deviations from a state grow exponentially in the course of time evolution. Therefore, as a first step, it is important to check whether the Bloch wave itself is stable against weak perturbations, which is the aim of this section.

We are interested in the parameter regime of strong lattice strength within the framework of the tight-binding approximation. Directly following Refs. [30–32], we proceed to expand the order parameters of $[\psi_1, \psi_2]^T$ in the Wannier basis and keep only the lowest vibrational states

as follows:

$$\psi_1 = \sqrt{N} \sum a_m(t) \phi(x - x_{1,m}), \quad (4)$$

$$\psi_2 = \sqrt{N} \sum_m^m b_m(t) \phi(x - x_{2,m}), \quad (5)$$

where $\phi(x - x_{i,m})$ is a Wannier function at the m sites and $x_{i,m}$ represents the central position of the i component at the m site.

In a similar way, Eq. (3) can be rewritten as under the tight-binding approximation,

$$i \frac{\partial}{\partial t} \alpha = (\Omega_m - i\gamma) \alpha - Q \sum_n |a_m|^2, \quad (6)$$

with

$$Q = \lambda N^{3/2} \int dx \sin(2x) |\phi(x - x_{1,m})|^2. \quad (7)$$

We focus on the stationary of the membrane by letting $\partial \alpha / \partial t = 0$ in Eq. (6). In such, we can obtain the value of the steady state α_0 and then the coupling strength between BEC and the membrane is connected to the real part of α_0 . By substituting the steady state of Eq. (6) into Eq. (1), we arrive at

$$i\hbar \frac{\partial \psi_1}{\partial t} = -\omega_R \partial_x^2 \psi_1 + V \sin^2(x) \psi_1 + gN |\psi_1|^2 \psi_1 + \Omega \psi_2 + g_{12} N |\psi_2|^2 \psi_1 - \frac{2\sqrt{N}\lambda Q}{\Omega_m} \sum_m |a_m|^2 \sin(2x) \psi_1. \quad (8)$$

Two properties of the effects of the backaction of the membrane on the quantum gas can immediately be stated based on Eq. (8): (i) This effective lattice with the renormalized lattice strength shares the same periodicity; (ii) its lattice site location is shifted from that of the original lattice, $x_m^{(0)} = ma_L$ ($m = 0, 1, 2, \dots$), to $x_m = ma_L + \delta$ by δ . The backaction of the membrane on the quantum gas is to provide the competition between the optical lattice, trying to localize the atoms at the minima, and the membrane displacement which tries to shift the atoms.

Furthermore, by plugging Eqs. (4) and (5) into Eqs. (8) and (2), we can obtain the discrete nonlinear Schrödinger equations as follows:

$$i\hbar \frac{\partial}{\partial t} a_m = -K_1 (a_{m-1} + a_{m+1}) + \Omega_{12} b_m + (\epsilon_{1,m} + U_{1,m} |a_m|^2 + U_{12} |b_m|^2) a_m, \quad (9)$$

$$i\hbar \frac{\partial}{\partial t} b_m = -K_2 (b_{m-1} + b_{m+1}) + \Omega_{12} b_m + (\epsilon_{2,m} + U_{2,m} |b_m|^2 + U_{12,m} |a_m|^2) b_m, \quad (10)$$

where

$$K_i = - \int \left[\omega_R \frac{\partial}{\partial x} \phi_{i,m} \frac{\partial}{\partial x} \phi_{i,m+1} + V \sin^2 x \phi_{i,m} \phi_{i,m+1} \right] dx \quad (11)$$

is the nearest neighbor hopping,

$$\epsilon_{i,m} = \frac{1}{2} \int \left[\omega_R \left| \frac{\partial}{\partial x} \phi_{i,m} \right|^2 + V \sin^2 x |\phi_{i,m}|^2 \right] dx \quad (12)$$

is the effective potential on every site, $U_{2,m} = \frac{gN}{2} \int |\phi_{2,m}|^4 dx$ is the on-site atomic collisions, $U_{12,m} = gN \int |\phi_{1,m}|^2 |\phi_{2,m}|^2 dx$ and $U_{1,m}$ can be adjusted by α_0 and λ with

$$U_{1,m} = \frac{gN}{2} \int |\psi_{1,m}|^4 dx - \frac{2N^2 \lambda^2}{\Omega_m} \int \sin(2x) |\phi(x - x_{1,m})|^2 dx \times \int \sum_m \sin(2x) |\phi(x - x_{1,m})|^2 dx. \quad (13)$$

The first term in Eq. (13) comes from the intrinsic interatomic interaction while the second term can be understood as the backaction of the shaking membrane on the interaction. It is expected because the effects of the backaction of the shaking membrane on the interaction should be weaker than the effects due to the intrinsic interatomic interaction, i.e., the value of the first term in Eq. (13) should be bigger than the second one. Indeed, in our detailed calculation, we always find $U_{1,m} > 0$.

$$M = \begin{pmatrix} h_1 & U_m n_0 & U_{12} n_0 + \Omega_{12} & U_{12} n_0 \\ -U_m n_0 & -h_1 & -U_{12} n_0 & -U_{12} n_0 - \Omega_{12} \\ U_{12} n_0 + \Omega_{12} & U_{12} n_0 & h_2 & U n_0 \\ -U_{12} n_0 & -U_{12} n_0 - \Omega_{12} & -U n_0 & -h_2 \end{pmatrix}. \quad (16)$$

Here, h_a and h_b are diagonal terms of the matrix, reading

$$h_i = 2K_i [\cos(k+q) + \cos(k)] + n_0 U_i - \Omega_{12}. \quad (17)$$

In some parameter regions, the imaginary parts of the eigenvalues of Eq. (16) are positive and the condensate wave functions with the form of Bloch waves come to be dynamically unstable, i.e., the density modulations grow in time exponentially. Stability phase diagrams of the spinor quantum gas in a lattice coupled to a membrane in the tight-binding limit are plotted in Fig. 1. In the white-color regions of Fig. 1, the imaginary parts of the dispersion spectrum for excitations of a Bloch wave are positive, suggesting dynamical instability of the condensate. These regimes correspond to effectively attractive nonlinearity of two-component GP equations as explained in Refs. [26,33]. Consequently, the growth of the spatial density modulations is supposed to lead to the formation of steady states with modulated density, which goes beyond the scope of current work. In what follows, we restrict our consideration to the dynamics of nonlinear waves propagating on a dynamically stable condensate background. Therefore we make sure that the parameters of the system always satisfy the dynamical stability condition.

IV. NONEQUILIBRIUM QUANTUM PHASE TRANSITION

The goal of this section is to investigate the nonequilibrium quantum phase transition based on Eqs. (1)–(3). At the heart of our solution of nonequilibrium dynamics of the spinor hybrid mechanical-atomic system is (i) an elimination of the degrees of freedom for the membrane, leading to an effective Lagrangian where the parameters are significantly renormalized by the atom-membrane coupling; (ii) the order parameters of the phases are calculated based on a Gaussian condensate profile.

The condition of the dynamical instabilities of Bloch waves solution can be determined based on Eqs. (9) and (10) as follows: We start from the standard decomposition of the wave functions into the steady-state solution labeled by the Bloch wave number k and a small fluctuating term with q being also a kind of Bloch wave number,

$$a_m = (\psi_{10} + u_1 e^{iqm-i\omega t} + v_1^* e^{-iqm+i\omega t}) e^{ikm-i\mu t}, \quad (14)$$

$$b_m = (\psi_{20} + u_2 e^{iqm-i\omega t} + v_2^* e^{-iqm+i\omega t}) e^{ikm-i\mu t}, \quad (15)$$

with $\psi_{10} = \psi_{20} = \sqrt{n_0}/2$ and considering one site with $U_{12,m} = U_{12}$, $U_{2,m} = U$, and $U_{1,m} = U_m$. Substituting Eqs. (14) and (15) into Eqs. (9) and (10) and retaining only first-order terms of fluctuation, we obtain at each momentum k the Bogoliubov–de Gennes (BdG) equation $M_k U_k = \hbar \omega_k U_k$ with $U_k = (u_1, v_1, u_2, v_2)^T$. Here the M_k in the matrix form reads as

We plan to develop a variational technique to analyze the nonequilibrium quantum phase transition. The basic idea behind the variational method is to take a trial function with a fixed shape, but with some free (time-dependent) parameters. Using a variational principle, we find a set of Newton-like ordinary differential equations for these parameters which characterize the solution. This technique has been used to study the nonequilibrium quantum phase transition of a hybrid atom-optomechanical system based on the one-component Gross-Pitaevskii equation coupled to a quantum oscillator [5].

The Lagrangian density of the hybrid system can be directly inferred from the effective Hamiltonian, reading

$$\begin{aligned} \mathcal{L} = & \frac{1}{V} \left[\frac{i\hbar}{2} (\partial_t \alpha \alpha^* - \alpha \partial_t \alpha^*) - \hbar \Omega_m \alpha^* \alpha \right] \\ & + \frac{i\hbar}{2} (\Psi^\dagger \partial_t \Psi - \partial_t \Psi^\dagger \Psi) \\ & - \frac{N}{4} [(g + g_{12}) \Psi^\dagger \Psi^\dagger \Psi \Psi + (g - g_{12}) \Psi^\dagger \Psi^\dagger \sigma_z \Psi \Psi] \\ & - [\omega_R |\partial_x \Psi|^2 + V \sin^2(x) \Psi^\dagger \Psi] \\ & - 2\sqrt{N} \lambda \alpha_1 \sin(2x) |\psi_1|^2 + \hbar \Omega \Psi^\dagger \sigma_x \Psi. \end{aligned} \quad (18)$$

Because the lattice potential can be approximately treated as a harmonic potential in each well, we are motivated to write the order parameters of the model system as Gaussian profile,

$$\psi_1 = \cos \theta(t) \left[\frac{1}{\pi \sigma(t)^2} \right]^{1/4} e^{-\frac{(x-\xi_1(t))}{2\sigma(t)^2} - ik(t)x - i\beta(t)x^2}, \quad (19)$$

$$\psi_2 = \sin \theta(t) \left[\frac{1}{\pi \sigma(t)^2} \right]^{1/4} e^{-\frac{(x-\xi_2(t))}{2\sigma(t)^2} - ik(t)x - i\beta(t)x^2}. \quad (20)$$

In this work, we are limited to the following cases: (i) two Gaussian wave packets have the same width $\sigma(t)$ with the

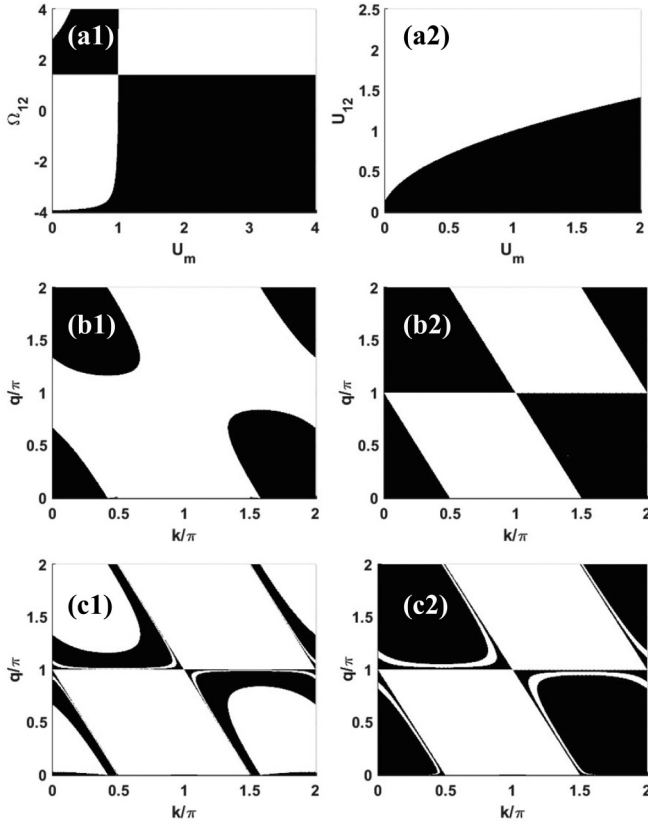


FIG. 1. Dynamical instability of a spinor quantum gas in a lattice coupled to a membrane. In the black-color regions, imaginary parts of dispersion spectrum for excitations of a Bloch wave are zero or negative, representing dynamical stability regions; while in the white-color regions, imaginary parts of dispersion spectrum for excitations of a Bloch wave are positive, suggesting dynamical instability of the condensate. Parameters are chosen as $K_1 = K_2 = 1$, and (a1) $k = \pi/4$, $q = 0$, $U_{12}/U = 1$; (a2) $k = \pi/4$, $q = 0$, $\Omega_{12}/U n_0 = 0$; (b1) $U_{12}/U = 1$, $\Omega/U n_0 = 0.5$, $U_m/U = 1.2$; (b2) $U_{12}/U = 1$, $\Omega/U n_0 = 0.5$, $U_m/U = 1.0$; (c1) $U_{12}/U = 1$, $\Omega/U n_0 = 0.5$, $U_m/U = 0.8$; and (c2) $U_{12}/U = 1$, $\Omega/U n_0 = 2$, $U_m/U = 0.8$.

corresponding phases $\beta(t)$ and $\kappa(t)$, suggesting that both condensate components oscillate in the phase; (ii) the centered positions of the two Gaussian wave packets are different, labeled $\zeta_1(t)$ and $\zeta_2(t)$, respectively. Note that all the parameters of θ , ζ , σ , κ , and β are all time-dependent variables. Our strategy of determining these parameters is as follows. First, we write down the equations of motion of ζ , σ , κ , and β with the help of the Euler-Lagrange equation. Second, we obtain the energy functional of the model system [see Eq. (26) below], which are a function of time-dependent parameters of θ , σ , and ζ . Finally, all these time-dependent parameters are numerically determined by minimizing the energy functional (26) below.

With the help of the trial functions of Eqs. (19) and (20), we can proceed to obtain the Lagrangian of the model system given by $L = \int \mathcal{L} dx$. Then, using the Euler-Lagrange equation, $\frac{\partial}{\partial t} \frac{\partial L}{\partial \dot{\xi}} - \frac{\partial L}{\partial \xi} = 0$ for the different parameter ξ , we can arrive at the equations of motion for the different parameters

β and κ as follows:

$$\zeta'_i = 2\omega_R(\kappa + 2\beta\zeta_i)(i = 1, 2), \quad (21)$$

$$\sigma' = 4\omega_R\beta\sigma. \quad (22)$$

Next, we can proceed to obtain the equations of motion for real number α_1 and the imaginary number α_2 , respectively,

$$\Omega_m\alpha_1 - \lambda\sqrt{N}\cos^2(\theta)e^{-\sigma^2}\sin(2\zeta_1) + \alpha'_2 = 0, \quad (23)$$

$$\Omega_m\alpha_2 - \alpha'_1 = 0. \quad (24)$$

By substituting Eq. (24) into Eq. (23), we can obtain the equation of motion of α_1 as follows:

$$\frac{\alpha''_1 + 2\gamma\alpha'_1}{\Omega_m} = \lambda\sqrt{N}\cos^2\theta e^{-\sigma(\sigma')^2}\sin(2\zeta_1) - \Omega_m\alpha_1. \quad (25)$$

Inspired by Ref. [5], we calculate the effective energy functional of the atom part as follows:

$$\begin{aligned} E = & \tilde{\Omega}_m\alpha_1^2 - 2\lambda\sqrt{N}\cos^2(\theta)\alpha_1 e^{-\sigma^2}\sin(X_0 + X_1) \\ & - \frac{Ve^{-\sigma^2}(\cos X_0 \cos X_1 - \cos(2\theta)\sin X_0 \sin X_1)}{2} \\ & + \frac{\omega_R}{2\sigma^2} + \Omega\sin(2\theta)e^{-\frac{X_1^2}{4\sigma^2}} + V/2 \\ & + \frac{Ng(\cos(4\theta) + 3) + 2Ng_{12}\sin^2(2\theta)e^{-\frac{X_1^2}{2\sigma^2}}}{8\sqrt{2\pi}\sigma}. \end{aligned} \quad (26)$$

Note that two-component BECs have different positions; we can use centered position $X_0 = \zeta_1 + \zeta_2$ and relative position $X_1 = \zeta_1 - \zeta_2$. In the similar way of Ref. [5], the equations of motion related to the condensate can be written as

$$\frac{X''_0}{2\omega_R} = -\partial_{X_0}E, \quad (27)$$

$$\frac{X''_1}{2\omega_R} = -\partial_{X_1}E, \quad (28)$$

$$\frac{\sigma''}{4\omega_R} = -\partial_\sigma E. \quad (29)$$

In determining the stationary-state phase diagram and the corresponding nonequilibrium phase transition of the energy functional (26), our strategy is based on the existence of four order parameters: the center-of-mass coordinate X_0 , the relative coordinate X_1 , the width of the wave packet σ , and the longitudinal spin polarization $\langle\sigma_z\rangle$. Depending on the interplay among the three order parameters, we identify two phases in the stationary-state phase diagram as follows.

Phase I is the localized symmetric phase, where both the center-of-mass coordinate X_0 and the relative coordinate X_1 are equal to zero and the longitudinal spin polarization $\langle\sigma_z\rangle = 0$. The stationary state is the superposition of two same Gaussian functions centered in the lattice wells.

Phase II is the localized symmetry-broken phase, where both the center-of-mass coordinate X_0 and the relative coordinate X_1 are equal to nonzero and the longitudinal spin polarization $\langle\sigma_z\rangle \neq 0$. The stationary state is the superposition of two of the same Gaussian functions with a shifted atom configuration in the lattice wells.

Below we drive the complete stationary-state phase diagram by numerically minimizing the energy functional (26).

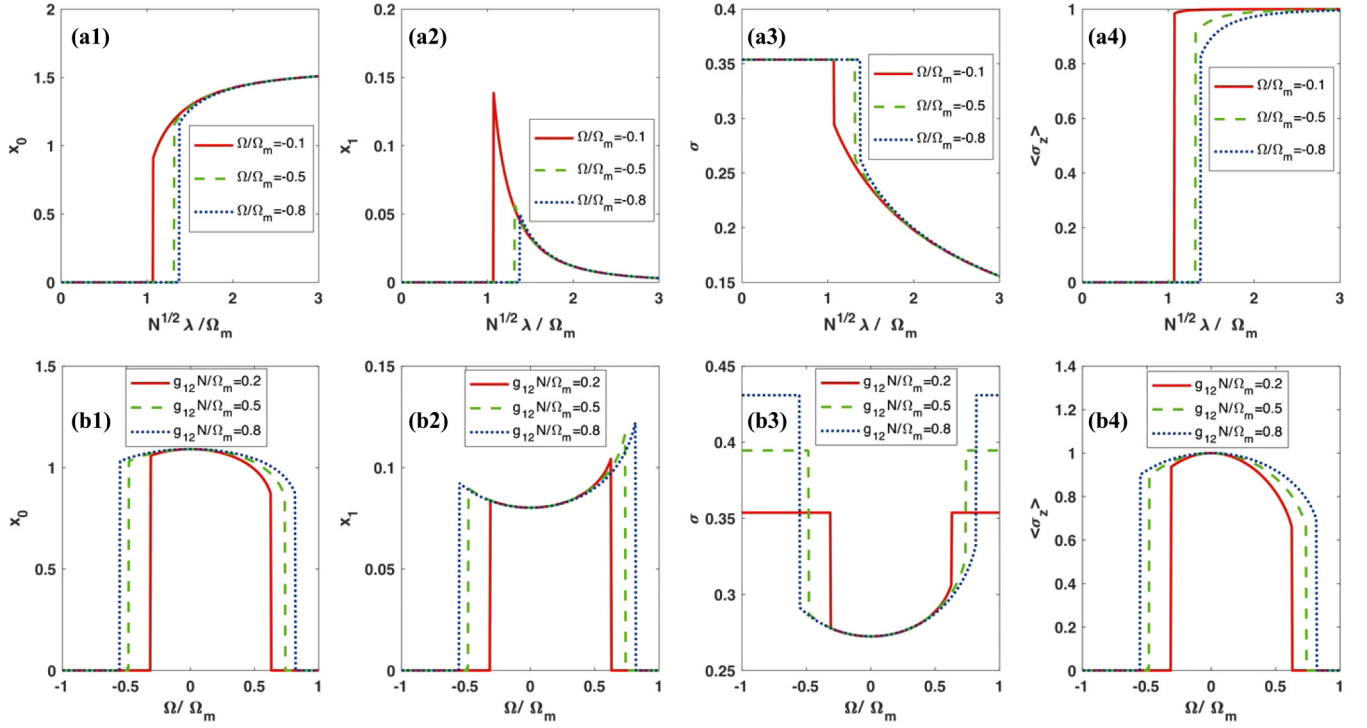


FIG. 2. Different parameters as a function of coupling strength (a1)–(a4) and Rabi frequency (b1)–(b4). Values of (a1) and (b1) centered positions of two wave packets; (a2) and (b2) relative position; (a3) and (b3) condensate width; and (a4) and (b4) $\langle \sigma_z \rangle = n_1 - n_2$ transform from zero to nonzero. The following parameters are used: $\Omega_m/\omega_R=100$, $gN/\Omega_m=0.3$, $V/\Omega_m=2$, $\gamma_R/\omega_R=20$; (a1)–(a4) $g_{12}N/\Omega_m=0.2$; and (b1)–(b4) $\lambda N^{1/2}/\Omega_m=1.2$.

After the ansatz of Eqs. (19) and (20) are determined, we accordingly calculate the center-of-mass coordinate X_0 , the relative coordinate X_1 , the width σ , and the longitudinal spin polarization $\langle \sigma_z \rangle \neq 0$. To comprehensively reveal the effects of the system's parameters, including the λ and Ω , on the nonequilibrium quantum phase transition from a localized symmetric state of atom cloud to a shifted symmetry-broken state, we have considered two cases for numerical analysis. (i) As is shown in Figs. 2(a1)–2(a4) the two-component hybrid system also has phase transition along with increasing coupling strength $\lambda\sqrt{N}$, centered position X_0 and polarized parameter $\langle \sigma_z \rangle$ turn from zero to nonzero, and relative position turns from zero to nonzero and then to zero. (ii) In Figs. 2(b1)–2(b4) when the coupling strength is fixed, Rabi frequency can control the phase transition, which brings a method to cool the membrane. Parameters have a jump at the critical point, which indicates the first-order transition because two-component condensates are nonequal and this progress happens discontinuously. If Rabi frequency is zero, the second component will vanish; for this reason in Figs. 1(b1)–1(b4) we ignore this case. For two components that have a different role, when adjusting Ω the phase transition is asymmetric.

V. HYSTERESIS AND LANDAU EXPANSION

In the previous section, we have found a NQPT of the hybrid atom-optomechanical systems. In this section, directly following Ref. [19], we plan to use the concepts of hysteresis

and Landau expansion to check whether such a NQPT studied in this work is the first-order one. Our strategy is as follows: Every order parameter of a first-order NQPT must have a jump at the critical point; therefore the occurrence of the hysteresis and the position of minimums of the Landau expansion can be treated as the characteristic features of the first-order quantum phase transition.

There will exist a hysteresis in the first-order quantum phase transition when the system Hamiltonian changes adiabatically. In this paper, we will focus on how the atom-membrane coupling of λ and Rabi frequency Ω can induce a first-order NQPT by monitoring the existence of a hysteresis. In this end, we take the time-dependent $X_1(t)$ as the order parameter and monitor how the values of $X_1(t)$ vary with the adiabatical change of the atom-membrane coupling of λ and Rabi frequency Ω by numerically solving Eqs. (27)–(29). As a comparison, we are also interested in the value of $X_1(\infty) = \lim_{t \rightarrow \infty} X_1(t)$ which becomes time independent. In more detail, we plot the hysteresis of the order parameter of $X_1(t=0)$ as the functions of λ and Ω in Figs. 3(a1) and 3(a2), respectively. It is clear that the forward path of the hysteresis is different from the backward one as is expected. The existence of the hysteresis curves suggests that the NQPT studied in this work is a first-order quantum phase transition, which can further be explained by the following results of the Landau expansion.

In order to understand the the hysteresis curves of X_1 as the functions of λ and Ω in Figs. 3(a1) and 3(a2), we take the energy functional of $E(X_1)$ in Eqs. (27)–(29) as the Taylor

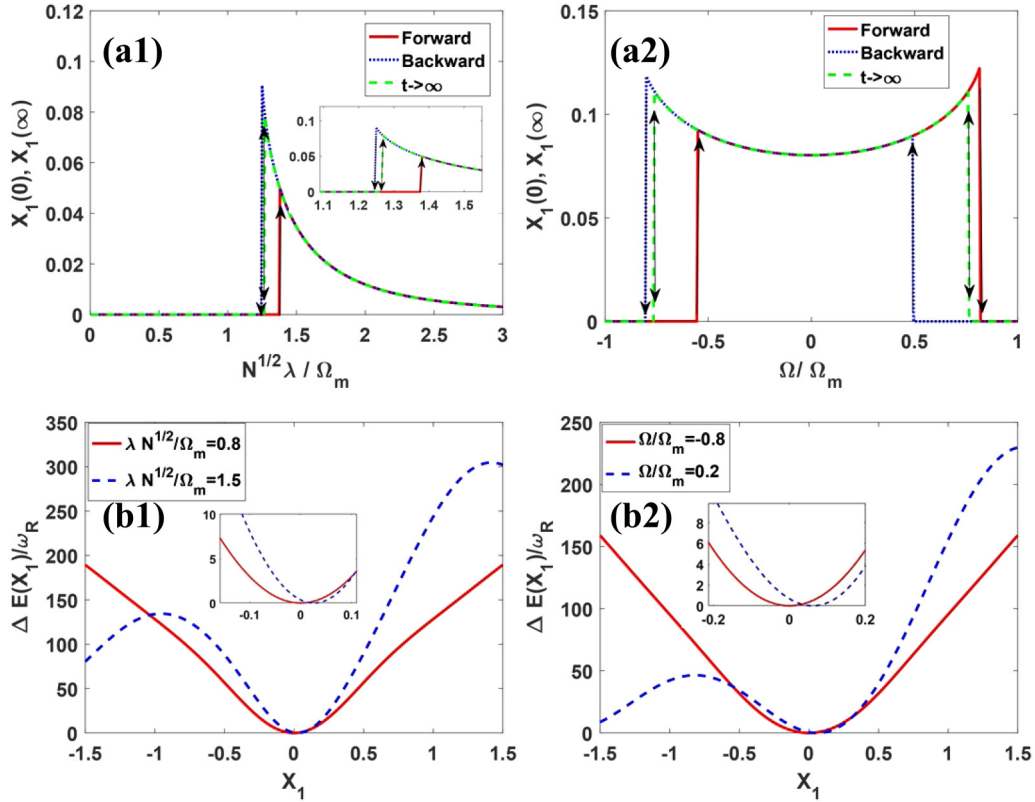


FIG. 3. Hysteresis curves of the first-order phase transition are shown as a function of the coupling parameter λ in (a1) and a function of Rabi frequency in (a2). (b1) and (b2) Curves of the effective energy difference $\Delta E(X_1) = E(X_1) - E(X_{10})$ are shown for a coupling strength and Rabi frequencies below and above the critical points. The following parameters are used: $\Omega_m/\omega_R=100$, $gN/\Omega_m=0.3$, $V/\omega_m=2$, $\gamma_R/\omega_R=20$; (a1) $g_{12}N/\Omega_m=0.2$, $\Omega/\Omega_m=-0.8$; and (a2) $g_{12}N/\Omega_m=0.8$, $\lambda N^{1/2}/\Omega_m=1.2$. The coefficients of a_i ($i = 0, 1, 2, \dots$) of Eq. (30) are shown in Appendix B.

expansion of X_1 as follows:

$$E(X_1) = a_0 + \sum_{n \geq 2} a_n X_1^n. \quad (30)$$

As pointed out by Ref. [19], in general, the coefficients a_n in Eq. (30) can also allow odd orders in n besides even orders in n . Here, θ , σ , X_0 , and X_1 are independent, so we cannot just use one parameter to clarify the phase transition. However, we can assume these parameters are around their steady state θ_0 , σ_0 , X_{00} , and X_{10} . Meanwhile, we will change the value of X_1 and fix the other parameters to investigate the dynamical instability. Finally, we will just use the numerical method of curve fitting to get the coefficients of the expansion coefficients of the Landau expansion of Eq. (30).

In Figs. 3(b1) and 3(b2), we find the system has the minimum at $X_1=0$ and the energy function of $E(X_1)$ is symmetry as a function of X_1 as shown in Eqs. (B1) and (B3) in Appendix B when the membrane-atom coupling strength is small or the Rabi frequency is large enough. Along with the increase of membrane-atom coupling strength and the decrease of the Rabi frequencies, the odd orders of expanding coefficients turn from zero to nonzero as shown in Eqs. (B2) and (B4) in Appendix B, which indicates $X_1 = 0$ points become unstable and asymmetric [see insets in Figs. 3(b1) and 3(b2)].

VI. ELEMENTARY EXCITATION

In this section, we proceed to discuss how the stationary-state phase can be revealed in elementary excitations by solving Eqs. (25)–(29) with the framework of the linear perturbation theory [28,34–36]. After obtaining the stationary states of $(\alpha_{10}, X_{00}, X_{10}, \sigma_0)$ in Eqs. (25)–(29), we proceed to calculate the collective spectrum by considering derivations from the stationary states in the form of $\alpha_{10} + \delta\alpha_{10}(t)$, $X_{00} + \delta X_{00}(t)$, $X_{10} + \delta X_{10}(t)$, $\sigma_0 + \delta\sigma(t)$. Then we substitute the solutions to motion equations and rewrite differential equations in the form of vector-matrix multiplications $\dot{v} = Mv$ with $v = (\delta\alpha_{10}, \delta X_{00}, \delta X_{10}, \delta\sigma)$. With defining the following useful constants,

$$\omega_1 = \lambda\sqrt{N}e^{-\sigma_0^2} \cos(X_{10} + X_{00}), \quad (31)$$

$$\omega_2 = \lambda\sqrt{N}e^{-\sigma_0^2} \sin(X_{10} + X_{00}), \quad (32)$$

$$\omega_{a1} = e^{-\sigma_0^2} V \cos(X_{00}) \cos(X_{10}), \quad (33)$$

$$\omega_{a2} = e^{-\sigma_0^2} V \cos(X_{00}) \sin(X_{10}), \quad (34)$$

$$\omega_{b1} = e^{-\sigma_0^2} V \sin(X_{00}) \sin(X_{10}), \quad (35)$$

$$\omega_{b2} = e^{-\sigma_0^2} V \sin(X_{00}) \cos(X_{10}), \quad (36)$$

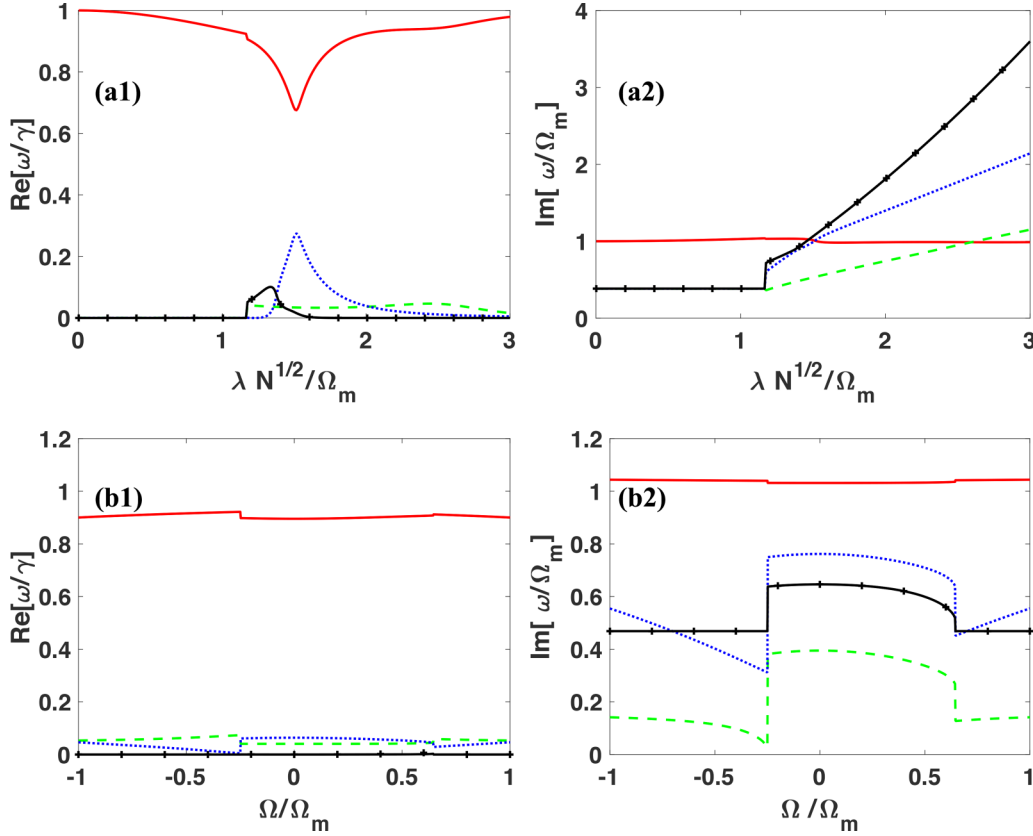


FIG. 4. Collective excitations of a spinor quantum gas in a lattice coupled to a membrane. (a1) and (b1) Real and (a2) and (b2) imaginary parts of excitations, respectively. (a1) and (a2) Elementary excitation energy as a function of coupling strength λ ; (b1)–(b2) elementary excitation energy as a function of Rabi frequency Ω . The following parameters are used: $\Omega_m/\Omega_R = 100$, $gN/\Omega_m = 0.3$, $g_{12}N/\Omega_m = 0.2$, $V/\Omega_m = 2$, $\gamma/\omega_R = 20$; (a1) and (a2) $\Omega/\Omega_m = -0.3$; (b1) and (b2) $\lambda\sqrt{N}/\Omega_m = 1.2$.

we finally obtain the matrix corresponding to the Bogoliubov–de Gennes [28,36] equation, reading

$$M = \begin{pmatrix} 0 & 1 & 0 & 0 & 0 & 0 & 0 & 0 & 0 \\ -\gamma^2 - \Omega_m^2 & -2\gamma & \omega_1 \cos^2(\theta)\Omega_m & 0 & \omega_1 \cos^2(\theta)\Omega_m & 0 & -2\sigma_0\omega_2 \cos^2(\theta)\Omega_m & 0 & 0 \\ 0 & 0 & 0 & 1 & 0 & 0 & 0 & 0 & 0 \\ 8\omega_1\omega_R & 0 & -4\omega_R(2\alpha_{10}\omega_2 + \omega_a) & 0 & \omega_{x01} & 0 & \omega_{x02} & 0 & 0 \\ 0 & 0 & 0 & 0 & 0 & 1 & 0 & 0 & 0 \\ 8\omega_1\omega_R & 0 & 4\omega_R(\omega_b - 2\alpha_{10}\omega_2) & 0 & \omega_{x11} & 0 & \omega_{x12} & 0 & 0 \\ 0 & 0 & 0 & 0 & 0 & 0 & 0 & 0 & 1 \\ -16\omega_2\sigma_0 \cos^2(\theta)\omega_R & 0 & \omega_{\sigma 1} & 0 & \omega_{\sigma 2} & 0 & \omega_{\sigma 3} & 0 & 0 \end{pmatrix}. \quad (37)$$

The real and imaginary parts of eigenvalues of the matrix (37) define the eigenfrequencies and the decay rates, respectively. In order to understand the effects of the system's parameters, including the λ and Ω , on the nonequilibrium quantum phase transition in terms of the collective excitations, we consider the following two cases: (i) We first fix the values of Ω and check how the collective excitations change with varying the values of λ . As shown in Figs. 4(a1) and 4(a2), the elementary excitations develop a jump at a critical point which is corresponding to the nonequilibrium quantum phase transition. (ii) As shown in Figs. 4(b1) and 4(b2), similar jumps of the excitations occur when the Ω can induce nonequilibrium quantum phase transition. As pointed out in Ref. [5], such kinds of jumps in excitation can be used to probe the nonequilibrium quantum phase transition experimentally.

VII. CONCLUSION

Summarizing, motivated by the experimental work [1–3], in which a novel kind of hybrid atom-optomechanical system has been realized by coupling atoms in a lattice to a membrane, we have further taken into account the effects of the spinor degree of freedom of the atom part on the nonequilibrium phases of the hybrid atom-optomechanical system. In more detail, a nonequilibrium quantum phase transition from a localized symmetric state of the atom cloud to a shifted symmetry-broken state, in particular, the effects of spinor degree of freedom on the nonequilibrium quantum phase transition are analyzed. The experimental realization of our scenario amounts to controlling two parameters whose interplay underlies the physics of this work: the lattice strength

V and the effective atom-membrane coupling λ . With the state-of-the-art technology [2], the variation of V and λ can be reached by adjusting the laser power and cavity finesse. Moreover, one can adjust the value of λ independent on V by applying a second laser which is slightly misaligned with the first one generating an optical lattice of the same periodicity but shifted by $\pi/2$.

We remark that our theoretical framework of studying the nonequilibrium quantum phase transitions in this work is limited in the zero temperature. It is supposed that the backaction of the membrane vibration on the atoms may induce the possible temperature effect. In more detail, the vibration of the membrane will lead to the shaking of the lattice by being mediated by the exchange of sideband photons of the lattice laser; as a result, the temperature of the atoms will increase. As estimated in our previous work [16] with the typical experimental parameters, the heating effect induced by the backaction of the membrane vibration on the atoms can be safely ignored by estimating the ratio between the energy scale of the backaction of the membrane vibration on the atoms and chemical potential of the optically trapped quantum gas as $\hbar\lambda/\mu \propto 10^{-2}$ [1,7]. We hope our work may induce the further experimental interests of quantum gases in a lattice coupled to a membrane with emphasis on the effects of the spinor degree of freedom. We emphasize here that the mean-field treatment of the hybrid atom-optomechanical system is limited to the Born-Markovian approximation of coupling between a membrane and the atoms at the zero temperature. For further investigations at the finite temperature or beyond Born-Markovian approximation, the path-integral Monte Carlo simulation should be a reliable theoretical framework.

ACKNOWLEDGMENTS

We thank M. Reza Bakhtiari, Ying Hu, Chao Gao, Xi-anlong Gao, and Biao Wu for inspiring discussion. This work is supported by the key projects of the Natural Science Foundation of China (Grant No. 11835011), the Natural Science Foundation of China (Grant No. 11274315) and Youth Innovation Promotion Association CAS (Grant No. 2013125).

APPENDIX A: THE MATRIX ELEMENTS IN EQ. (37)

caps per style. The matrix elements in Eq. (37) are given as follows:

$$\begin{aligned} \omega_{x01}/\omega_R &= \frac{\sqrt{\frac{2}{\pi}} g_{12} N \cos(2\theta) e^{-\frac{x_{10}^2}{2\sigma_0^2}} (X_{10}^2 - \sigma_0^2)}{\sigma_0^5} + 4(\omega_b - 2\alpha_{10}\omega_2) \\ &+ \frac{2\Omega \cot(2\theta) e^{-\frac{x_{10}^2}{4\sigma_0^2}} (X_{10}^2 - 2\sigma_0^2)}{\sigma_0^4}, \end{aligned} \quad (\text{A1})$$

$$\begin{aligned} \omega_{x02}/\omega_R &= -\frac{\sqrt{\frac{2}{\pi}} g_{12} N \cos(2\theta) e^{-\frac{x_{10}^2}{2\sigma_0^2}} X_{10} (X_{10}^2 - 3\sigma_0^2)}{\sigma_0^6} \\ &+ 8\sigma_0(\omega_{b2} - 2\alpha_{10}\omega_1) \\ &- \frac{2\Omega \cot(2\theta) e^{-\frac{x_{10}^2}{4\sigma_0^2}} X_{10} (X_{10}^2 - 4\sigma_0^2)}{\sigma_0^5}, \end{aligned} \quad (\text{A2})$$

$$\begin{aligned} \omega_{x11}/\omega_R &= \frac{\sqrt{\frac{2}{\pi}} g_{12} N e^{-\frac{x_{10}^2}{2\sigma_0^2}} (\sigma_0^2 - X_{10}^2)}{\sigma_0^5} - 4(2\alpha_{10}\omega_2) + (\omega_a) \\ &+ \frac{\Omega \csc(\theta) \sec(\theta) e^{-\frac{x_{10}^2}{4\sigma_0^2}} (2\sigma_0^2 - X_{10}^2)}{\sigma_0^4}, \end{aligned} \quad (\text{A3})$$

$$\begin{aligned} \omega_{x12}/\omega_R &= \frac{\sqrt{\frac{2}{\pi}} g_{12} N \cos(2\theta) e^{-\frac{x_{10}^2}{2\sigma_0^2}} X_{10} (X_{10}^2 - 3\sigma_0^2)}{\sigma_0^6} \\ &+ 8\sigma_0(\omega_{a2} - 2\alpha_{10}\omega_1) \\ &+ \frac{\Omega \csc \theta \sec \theta e^{-\frac{x_{10}^2}{4\sigma_0^2}} X_{10} (X_{10}^2 - 4\sigma_0^2)}{\sigma_0^5}, \end{aligned} \quad (\text{A4})$$

$$\omega_{\sigma 1}/\omega_R = 4\sigma_0(-4\alpha_{10} \cos^2(\theta)\omega_1 + \cos(2\theta)\omega_{a2} + \omega_{b2}), \quad (\text{A5})$$

$$\begin{aligned} \omega_{\sigma 2}/\omega_R &= \frac{4g_{12} N \sin^2(\theta) \cos^2(\theta) e^{-\frac{x_{10}^2}{2\sigma_0^2}} X_{10} (X_{10}^2 - 3\sigma_0^2)}{\sqrt{2\pi}\sigma_0^6} \\ &+ 4\sigma_0(-4\alpha_{10} \cos^2(\theta)\omega_1 + \cos(2\theta)\omega_{b2} + \omega_{a2}) \\ &+ \frac{\Omega \sin(2\theta) e^{-\frac{x_{10}^2}{4\sigma_0^2}} X_{10} (X_{10}^2 - 4\sigma_0^2)}{\sigma_0^5}, \end{aligned} \quad (\text{A6})$$

$$\begin{aligned} \omega_{\sigma 3}/\omega_R &= -\frac{\sqrt{\frac{2}{\pi}} g N (\cos(4\theta) + 3)}{2\sigma_0^3} \\ &+ \frac{g_{12} N (\cos(4\theta) - 1) e^{-\frac{x_{10}^2}{2\sigma_0^2}} (2\sigma_0^4 + X_{10}^4 - 5\sigma_0^2 X_{10}^2)}{2\sqrt{2\pi}\sigma_0^7} \\ &+ 4(2\sigma_0^2 - 1)(4\alpha_{10} \cos^2(\theta)\omega_2 - \cos(2\theta)\omega_b + \omega_a) \\ &- \frac{12\omega_R}{\sigma_0^4} - \frac{\Omega \sin(2\theta) e^{-\frac{x_{10}^2}{4\sigma_0^2}} X_{10}^2 (X_{10}^2 - 6\sigma_0^2)}{\sigma_0^6}. \end{aligned} \quad (\text{A7})$$

APPENDIX B: LANDAU EXPANSION COEFFICIENTS IN FIG. 3

We use the numerical method of data fitting to obtain the coefficients of a_n in Eq. (30). For the symmetry-unbroken phase in Fig. 3(b1), the coefficients of the fitting curve polynomial function are

$$\begin{aligned} a_0 &= 1.143, & a_2 &= 2.711, & a_4 &= -238.1, & a_6 &= 114.4, \\ a_8 &= -20.38, & a_3 &= a_5 &= a_7 &= 0. \end{aligned} \quad (\text{B1})$$

For the symmetry-broken phase in Fig. 3(b2), the coefficients of the fitting curve polynomial function are

$$\begin{aligned} a_0 &= 3.645, & a_2 &= 412, & a_3 &= 45.87, & a_4 &= -348.5, \\ a_5 &= 16.19, & a_6 &= 146.2, & a_7 &= -10.1, & a_8 &= -25.19. \end{aligned} \quad (\text{B2})$$

For the symmetry-unbroken phase in Fig. 3(b2), the coefficients of the fitting curve polynomial function are

$$\begin{aligned} a_0 &= -0.2783, & a_2 &= 144.2, \\ a_4 &= -68.15, & a_6 &= 114.4, \\ a_8 &= -20.38, & a_3 &= a_5 = a_7 = 0. \end{aligned} \quad (\text{B3})$$

For the symmetry-broken phase in Fig. 3(b2), the coefficients of the fitting curve polynomial function are

$$\begin{aligned} a_0 &= 0.7595, & a_2 &= 164.8, & a_3 &= 56.68, & a_4 &= -86, \\ a_5 &= 4.558, & a_6 &= 21.75, \\ a_7 &= -7.016, & a_8 &= -2.531. \end{aligned} \quad (\text{B4})$$

-
- [1] A. Vochezer, T. Kampschulte, K. Hammerer, and P. Treutlein, Light-Mediated Collective Atomic Motion in an Optical Lattice Coupled to a Membrane, *Phys. Rev. Lett.* **120**, 073602 (2018).
- [2] A. Jöckel, A. Faber, T. Kampschulte, M. Korppi, M. T. Rakher, and P. Treutlein, Sympathetic cooling of a membrane oscillator in a hybrid mechanical–atomic system, *Nat. Nanotechnol.* **10**, 55 (2015).
- [3] P. Christoph, T. Wagner, H. Zhong, R. Wiesendanger, K. Sengstock, A. Schwarz, and C. Becker, Combined feedback and sympathetic cooling of a mechanical oscillator coupled to ultracold atoms, *New J. Phys.* **20**, 093020 (2018).
- [4] H. Ritsch, Atoms Oscillate Collectively in Large Optical Lattice, *Physics* **11**, 17 (2018).
- [5] N. Mann, M. R. Bakhtiari, A. Pelster, and M. Thorwart, Nonequilibrium Quantum Phase Transition in a Hybrid Atom-Optomechanical System, *Phys. Rev. Lett.* **120**, 063605 (2018).
- [6] S. Camerer, M. Korppi, A. Jöckel, D. Hunger, T. W. Hänsch, and P. Treutlein, Realization of an Optomechanical Interface between Ultracold Atoms and a Membrane, *Phys. Rev. Lett.* **107**, 223001 (2011).
- [7] B. Vogell, K. Stannigel, P. Zoller, K. Hammerer, M. T. Rakher, M. Korppi, A. Jöckel, and P. Treutlein, Cavity-enhanced long-distance coupling of an atomic ensemble to a micromechanical membrane, *Phys. Rev. A* **87**, 023816 (2013).
- [8] J. S. Bennett, L. S. Madsen, M. Baker, H. Rubinsztein-Dunlop, and W. P. Bowen, Coherent control and feedback cooling in a remotely coupled hybrid atom-optomechanical system, *New J. Phys.* **16**, 083036 (2014).
- [9] B. Vogell, T. Kampschulte, M. T. Rakher, A. Faber, P. Treutlein, K. Hammerer, and P. Zoller, Long distance coupling of a quantum mechanical oscillator to the internal states of an atomic ensemble, *New J. Phys.* **17**, 043044 (2015).
- [10] C. B. Møller, R. A. Thomas, G. Vasilakis, E. Zeuthen, Y. Tsaturyan, M. Balabas, K. Jensen, A. Schliesser, K. Hammerer, and E. S. Polzik, Quantum back-action-evading measurement of motion in a negative mass reference frame, *Nature (London)* **547**, 191 (2017).
- [11] F. Marquardt, D. München, and S. M. Girvin, Optomechanics (a brief review), *Physics* **2**, 40 (2009).
- [12] M. Aspelmeyer, T. J. Kippenberg, and F. Marquardt, Cavity optomechanics, *Rev. Mod. Phys.* **86**, 1391 (2014).
- [13] V. Sudhir, D. J. Wilson, R. Schilling, H. Schütz, S. A. Fedorov, A. H. Ghadimi, A. Nunnenkamp, and T. J. Kippenberg, Appearance and Disappearance of Quantum Correlations in Measurement-Based Feedback Control of a Mechanical Oscillator, *Phys. Rev. X* **7**, 011001 (2017).
- [14] J. G. E. Harris, Ambient quantum optomechanics, *Science* **356**, 1232 (2017).
- [15] V. D. Vaidya, Y. Guo, R. M. Kroeze, K. E. Ballantine, A. J. Kollár, J. Keeling, and B. L. Lev, Tunable-Range, Photon-Mediated Atomic Interactions in Multimode Cavity QED, *Phys. Rev. X* **8**, 011002 (2018).
- [16] C. Gao and Z. Liang, Steady-state phase diagram of quantum gases in a lattice coupled to a membrane, *Phys. Rev. A* **99**, 013629 (2019).
- [17] D. Jaksch and P. Zoller, The cold atom Hubbard toolbox, *Ann. Phys.* **315**, 52 (2005).
- [18] M. R. Bakhtiari, A. Hemmerich, H. Ritsch, and M. Thorwart, Nonequilibrium Phase Transition of Interacting Bosons in an Intra-Cavity Optical Lattice, *Phys. Rev. Lett.* **114**, 123601 (2015).
- [19] N. Mann, A. Pelster, and M. Thorwart, Tuning the order of the nonequilibrium quantum phase transition in a hybrid atom-optomechanical system, [arXiv:1810.12846](https://arxiv.org/abs/1810.12846).
- [20] D. M. Stamper-Kurn and M. Ueda, Spinor Bose gases: Symmetries, magnetism, and quantum dynamics, *Rev. Mod. Phys.* **85**, 1191 (2013).
- [21] F. Mivehvar, H. Ritsch, and F. Piazza, Cavity-Quantum-Electrodynamical Toolbox for Quantum Magnetism, *Phys. Rev. Lett.* **122**, 113603 (2019).
- [22] S. Ostermann, H.-W. Lau, H. Ritsch, and F. Mivehvar, Cavity-induced emergent topological spin textures in a Bose–Einstein condensate, *New J. Phys.* **21**, 013029 (2019).
- [23] H.-N. Dai, B. Yang, A. Reingruber, X.-F. Xu, X. Jiang, Y.-A. Chen, Z.-S. Yuan, and J.-W. Pan, Generation and detection of atomic spin entanglement in optical lattices, *Nat. Phys.* **12**, 783 (2016).
- [24] B. Yang, H.-N. Dai, H. Sun, A. Reingruber, Z.-S. Yuan, and J.-W. Pan, Spin-dependent optical superlattice, *Phys. Rev. A* **96**, 011602(R) (2017).
- [25] M. Abad and A. Recati, A study of coherently coupled two-component bose-einstein condensates, *Eur. Phys. J. D* **67**, 148 (2013).
- [26] X. Xu, Y. Hu, Z. Zhang, and Z. Liang, Spinor polariton condensates under nonresonant pumping: Steady states and elementary excitations, *Phys. Rev. B* **96**, 144511 (2017).
- [27] B. Wu and Q. Niu, Landau and dynamical instabilities of the superflow of Bose-Einstein condensates in optical lattices, *Phys. Rev. A* **64**, 061603(R) (2001).
- [28] W. Li, L. Chen, Z. Chen, Y. Hu, Z. Zhang, and Z. Liang, Probing the flat band of optically trapped spin-orbital-coupled Bose gases using Bragg spectroscopy, *Phys. Rev. A* **91**, 023629 (2015).
- [29] B. Wu and Q. Niu, Superfluidity of Bose–Einstein condensate in an optical lattice: Landau–Zener tunneling and dynamical instability, *New J. Phys.* **5**, 104 (2003).

- [30] Z. X. Liang, Xi Dong, Z. D. Zhang, and B. Wu, Sound speed of a Bose-Einstein condensate in an optical lattice, *Phys. Rev. A* **78**, 023622 (2008).
- [31] A. Trombettoni and A. Smerzi, Discrete Solitons and Breathers with Dilute Bose-Einstein Condensates, *Phys. Rev. Lett.* **86**, 2353 (2001).
- [32] D. Jaksch, C. Bruder, J. I. Cirac, C. W. Gardiner, and P. Zoller, Cold Bosonic Atoms in Optical Lattices, *Phys. Rev. Lett.* **81**, 3108 (1998).
- [33] L. A. Smirnov, D. A. Smirnova, E. A. Ostrovskaya, and Y. S. Kivshar, Dynamics and stability of dark solitons in exciton-polariton condensates, *Phys. Rev. B* **89**, 235310 (2014).
- [34] D. Nagy, G. Szirmai, and P. Domokos, Self-organization of a Bose-Einstein condensate in an optical cavity, *Eur. Phys. J. D* **48**, 127 (2008).
- [35] D. Nagy, P. Domokos, A. Vukics, and H. Ritsch, Nonlinear quantum dynamics of two BEC modes dispersively coupled by an optical cavity, *Eur. Phys. J. D* **55**, 659 (2009).
- [36] Z. Chen and Z. Liang, Ground-state phase diagram of a spin-orbit-coupled bosonic superfluid in an optical lattice, *Phys. Rev. A* **93**, 013601 (2016).